N 62 70814

NASA TN D-240

7N-02
198505
P-28

NASA TN D-240

TECHNICAL NOTE
D - 240

A NOTE ON THE MEAN VALUE OF INDUCED VELOCITY FOR A HELICOPTER ROTOR

By Harry H. Heyson

Langley Research Center
Langley Field, Va.

NATIONAL AERONAUTICS AND SPACE ADMINISTRATION

WASHINGTON May 1960

1T

NATIONAL AERONAUTICS AND SPACE ADMINISTRATION

TECHNICAL NOTE D-240

A NOTE ON THE MEAN VALUE OF INDUCED VELOCITY FOR A HELICOPTER ROTOR

By Harry H. Heyson

L
7
5
3

SUMMARY

A theoretical study shows the exact equivalence of momentum and vortex theory in the determination of the induced velocity at the rotor regardless of whether terms involving the sine of the azimuth angle are included in the blade circulation. It is shown that erroneous results may be incurred by failure to utilize a consistent set of assumptions in formulating the vortex-theory analysis. In particular, if the lateral dissymmetry on the rotor is represented by blade circulation which varies as the sine of the azimuth angle, it is then necessary to include the effect of the axial wake vorticity.

INTRODUCTION

Rotary-wing blade-element theory uses an interference velocity based upon the plausible momentum hypothesis offered in references 1 and 2. The only justification offered for this hypothesis was that in hovering the results coincided with those for a propeller, and that in high-speed forward flight the results coincided with those for a wing.

The simple vortex theory (such as that given in ref. 3) lends some additional credence to the momentum theory since the simple vortex theory and momentum theory can be shown to lead to precisely the same induced velocity.

A subsequent development of vortex theory (ref. 4), which attempts to account for dissymmetry of loading, yields a somewhat different result for the induced velocity. In this case, the induced velocity appears to increase with tip-speed ratio according to the factor $\dfrac{1}{1 - \frac{3}{2}\mu^2}$. This factor, of course, changes the induced velocity very little at current helicopter tip-speed ratios which are of the order of 0.3; however, it could have a large effect when applied to performance calculations for autogyros and convertiplanes which operate at much higher values of tip-speed ratio.

This paper studies the induced velocity of a uniformly loaded rotor in some detail with particular attention given to the velocity at the center of the rotor. In order to simplify the final comparison, the momentum theory derivation is also given. Then the vortex-theory derivations, both with symmetrical and asymmetrical circulation, are given, including for the first time, the effect of the axial vorticity in the wake. Finally, the correspondence between momentum and vortex theories is discussed.

The results indicate that certain groupings of assumptions form consistent sets when formulating the vortex theory and that failure to use a consistent set may lead to significant errors.

L758

SYMBOLS

$\bar{a}$	vector distance from point in space to vortex element, ft
b	number of blades
C_T	rotor-thrust coefficient, $\frac{T}{\rho\pi R^2(\Omega R)^2}$
$d\bar{s}$	vector length of vortex element, ft
$\bar{i},\bar{j},\bar{k}$	unit direction vectors along X-, Y-, and Z-axes, respectively
L	running coordinate along edge of wake, ft
M_T	thrust moment for blade, ft-lb
P	arbitrary point in space
$\bar{q}_a$	vector induced velocity caused by axial component of vorticity
r	radial distance to blade element, ft
R	rotor radius, ft
$\bar{s}$	vector from origin to point on wake, ft
T	rotor thrust, lb
U_T	tangential component of resultant velocity at blade element, $\Omega r + \mu\Omega R \sin\psi$, ft/sec

V	forward velocity of rotor, ft/sec
V'	resultant velocity at rotor, ft/sec
w	induced velocity, positive when directed upward, ft/sec
w_a	induced velocity contribution of axial component of vorticity, positive when directed upward, ft/sec
w_c	induced velocity contribution of circumferential (vortex-ring) component of vorticity, positive when directed upward, ft/sec
X,Y,Z	Cartesian axes centered in rotor
x,y,z	Cartesian coordinate system centered in rotor, x measured rearward, y laterally, and z upward, ft
α	rotor tip-path-plane angle of attack, radians
Γ	blade circulation, ft^2/sec
Γ_0	strength of constant part of blade circulation, ft^2/sec
Γ_1	strength of $\sin\psi$ part of blade circulation, ft^2/sec
ϵ	a small angle, radians
λ	rotor inflow ratio, nondimensional component of velocity perpendicular to rotor disk, $\frac{V \sin \alpha + w}{\Omega R}$
μ	rotor tip-speed ratio, nondimensional component of velocity parallel to rotor disk, $\frac{V \cos \alpha}{\Omega R}$
ρ	mass density of air, slugs/cu ft
χ	wake skew angle, angle between axis of wake and rotor tip-path-plane axis, $\tan^{-1} \frac{-\mu}{\lambda}$, deg
ψ	rotor azimuth angle, radians
Ω	rotor rotational speed, radians/sec

MOMENTUM THEORY

Momentum theory, as applied to helicopter rotors (refs. 1 and 2), assumes that the mass of air affected by the rotor is that which flows through a sphere (fig. 1) of radius R which is centered in the rotor. The velocity at the rotor is V' the resultant between the forward and induced velocities. This mass, per unit time, is

$$\frac{\text{Mass}}{\text{Time}} = \rho\pi R^2 V'$$

This mass is given a downward velocity of $-2w$ at an infinite distance along the wake, thus the thrust, which is equal to the time rate of change of momentum, is

$$T = -2\rho\pi R^2 V' w \tag{1}$$

Rewriting this equation yields

$$w = \frac{-T}{2\rho\pi R^2 V'}$$

which, in nondimensional terms, is

$$w = \frac{-\frac{1}{2} C_T \Omega R}{\sqrt{\mu^2 + \lambda^2}} \tag{2}$$

VORTEX THEORY

ASSUMED WAKE SHAPE

The wake assumed as a basis for the present vortex theory is shown for one blade in figure 2. The circulation Γ along the blade is considered as being radially uniform. (This restriction has been removed in the case of circular symmetry by ref. 5; however, the uniform circulation case considered herein yields values at the origin which are more nearly representative of the average induced velocity for the entire rotor.) Since the blade circulation is uniform, trailing vortices spring only from the blade tip and the blade root. These vortices are assumed to be carried off uniformly with the velocity and direction of the mean flow V'. Thus, the tip vortex forms a spiral on the surface of a skewed elliptic cylinder, and the root vortex lies along the center line of this cylinder.

At this point, the analysis is restricted to time-averaged induced velocities by assuming that the vortices are so closely spaced that they may be considered to form a continuous cylindrical sheet of vorticity. As in reference 3, this cylindrical sheet is now broken into its two components; one circumferential (vortex rings) and one axial. (See fig. 3.) The axial component of vorticity is neglected in references 3 and 4 on the basis that its effect is small. This component will, however, be considered in the present paper.

If, as in reference 4, the blade circulation and wake vorticity are allowed to vary with azimuth angle, the aforementioned vorticity will not be sufficient to describe the entire wake, since additional radial vorticity must now be shed from the trailing edge of the blades in order to compensate for the change in blade circulation. These radial vortices are illustrated in figure 4 for a simple case in which the blade circulation is uniformly increased over one sector of the rotor disk. In the present case, the blade circulation will be assumed to vary as $\sin \psi$, so that the radial vorticity will completely fill the wake cylinder and its strength will be proportional to $\cos \psi$.

STRENGTH OF CIRCULATION AND VORTICITY

Blade Circulation

<u>With varying circulation</u>.- Assume, as in reference 4, that the blade circulation is constant along the radius, but varies azimuthwise according to

$$\Gamma = \Gamma_0 + \Gamma_1 \sin \psi \tag{3}$$

Then, since

$$dT = \rho U_T \Gamma \, dr \tag{4a}$$

the rotor thrust will be

$$T = \frac{b}{2\pi} \int_0^{2\pi} \int_0^R \rho(\Omega r + \mu\Omega R \sin\psi)(\Gamma_0 + \Gamma_1 \sin\psi)\, dr\, d\psi \tag{4b}$$

Integrating equation (4b) yields

$$T = b\rho \frac{\Omega R^2}{2}\left(\Gamma_0 + \mu\Gamma_1\right) \tag{5}$$

or, nondimensionally,

$$C_T = \frac{b}{2} \frac{\Gamma_0 + \mu\Gamma_1}{\Omega\pi R^2} \tag{6}$$

The relation between Γ_0 and Γ_1 is determined, as in reference 4, from the thrust moment, which is

$$\begin{aligned} M_T &= \int_0^R \rho(\Omega r + \mu\Omega R \sin\psi)(\Gamma_0 + \Gamma_1 \sin\psi) r\, dr \\ &= \rho\Omega R^3 \left[\frac{\Gamma_0}{3} + \left(\frac{\Gamma_1}{3} + \frac{\mu\Gamma_0}{2}\right)\sin\psi + \frac{\mu\Gamma_1}{2}\sin^2\psi\right] \end{aligned} \tag{7}$$

Now, if only first harmonic flapping is significant, the first harmonic of the thrust moment must be zero (ref. 6); thus, from equation (7)

$$\Gamma_1 = -\frac{3}{2}\mu\Gamma_0 \tag{8}$$

so that, equation (6) becomes

$$C_T = \frac{b}{2} \frac{\left(1 - \frac{3}{2}\mu^2\right)}{\Omega\pi R^2} \Gamma_0 \tag{9}$$

and solving equations (8) and (9) for Γ_0 and Γ_1

$$\Gamma_0 = \frac{2C_T\Omega\pi R^2}{b\left(1 - \frac{3}{2}\mu^2\right)} \tag{10}$$

$$\Gamma_1 = -\frac{3}{2}\mu\frac{2C_T\Omega\pi R^2}{b\left(1 - \frac{3}{2}\mu^2\right)} \tag{11}$$

L
7
5
8

With only constant circulation.- If, as in reference 3, the circulation was constant $(\Gamma_1 = 0)$, the corresponding results would be

$$T = \frac{1}{2}b\rho\Omega R^2\Gamma_0 \tag{12}$$

$$C_T = \frac{b\Gamma_0}{2\Omega\pi R^2} \tag{13}$$

and

$$\Gamma_0 = \frac{2C_T\Omega\pi R^2}{b} \tag{14}$$

Central Vortex

The central vortex on the center of the wake cylinder is formed by the superposition of the root vortices of all blades; thus, its circulation strength is the sum of blade bound vortex strengths.

Circumferential Vorticity

With $\sin\psi$ circulation.- The number of circular vortex elements formed per unit time at the rotor disk is $b\Omega/2\pi$. These elements are carried off with the velocity $\Omega R\sqrt{\mu^2 + \lambda^2}$. Thus, the vorticity along the edge of the wake will be

$$\frac{d\Gamma}{dL} = \frac{d\Gamma_0}{dL} + \frac{d\Gamma_1}{dL} \sin \psi = (\Gamma_0 + \Gamma_1 \sin \psi)\frac{\frac{b\Omega}{2\pi}}{\Omega R\sqrt{\mu^2 + \lambda^2}}$$

So that

$$\frac{d\Gamma_0}{dL} = \frac{b\Gamma_0}{2\pi R\sqrt{\mu^2 + \lambda^2}} = \frac{C_T \Omega R}{\left(1 - \frac{3}{2}\mu^2\right)\sqrt{\mu^2 + \lambda^2}} \tag{15}$$

L
7
5
8

and

$$\frac{d\Gamma_1}{dL} = \frac{b\Gamma_1}{2\pi R\sqrt{\mu^2 + \lambda^2}} = \frac{-\frac{3}{2}\mu C_T \Omega R}{\left(1 - \frac{3}{2}\mu^2\right)\sqrt{\mu^2 + \lambda^2}} \tag{16}$$

With only constant circulation.- For the corresponding case of uniform circulation

$$\frac{d\Gamma_0}{dL} = \frac{C_T \Omega R}{\sqrt{\mu^2 + \lambda^2}} \tag{17}$$

Axial Vorticity

High-speed forward flight is the only condition under which the $\frac{1}{1 - \frac{3}{2}\mu^2}$ term of reference 4 has a significant effect. Thus, in the present analysis, the axial vorticity will be considered only for the corresponding condition, $\chi = 90^\circ$, where the wake is assumed to flow directly rearward in the same plane as the rotor. This, as will be seen later, results in a major simplification of the analysis.

The wake is shown in plan view at $\chi = 90^\circ$ in figure 5(a). The locus of the tip of any one blade as the rotor moves forward is a cycloid rather than a circle. Furthermore, relative to the rotor, the tip vortex also lies on this cycloid. This is shown in the figure for one revolution starting at $\psi = \pi$. If the shaded area of figure 5(a) is developed into a plane triangle, figure 5(b) results. The axial and circumferential vorticities $d\Gamma/d(R\psi)$ and $d\Gamma/dL$ are in the same proportion as the sides of the triangle. Thus, the axial vorticity is

$$\frac{d\Gamma}{d(R\psi)} = \mu\left[\frac{d\Gamma_0}{dL} + \frac{d\Gamma_1}{dL}\sin\psi\right] \tag{18}$$

where $d\Gamma_0/dL$ and $d\Gamma_1/dL$ are given by equations (15) and (16).

Radial Vorticity

The strength of the radial vorticity is simply the derivative of the strength of the circumferential vorticity, or

$$\frac{d}{d\psi}\left[\frac{d\Gamma}{dL}\right] = \frac{d\Gamma_1}{dL}\cos\psi \tag{19}$$

INDUCED VELOCITY CONTRIBUTIONS OF THE VARIOUS COMPONENTS OF THE WAKE

Blade Circulation

Constant term.- In figure 6, consider any point P in the space surrounding the rotor and also a plane which contains both this point and the Z-axis. At some blade position, say 1, the blade vortex induces a velocity at P. In the course of its revolution the blade later passes the symmetrical position 2. Here it induces a velocity equal and opposite to that which it induced when at 1. Considering all symmetrical positions it is thus evident that, on a time-averaged basis (or equally as well, for an infinite number of blades) the contribution of constant blade circulation is zero.

Sin ψ term.- The argument for the $\sin\psi$ term is identical to that used in the previous section, except that P in figure 6 must now be considered as confined to the Y-Z plane, about which $\sin\psi$ is symmetrical. This plane, which includes the center and the lateral axis, will have no induced velocity caused by the $\sin\psi$ blade circulation. There will be an induced velocity at other points on the rotor disk. These induced velocities will be antisymmetric about the lateral axis. Thus, for the $\sin\psi$ part of the blade circulation, the average induced velocity over the disk, as well as the induced velocity at the center, is zero.

Central Vortex

Since the central vortex lies in the same plane as the longitudinal axis, it will not induce a vertical velocity at any point on this axis. Notice that the $\sin \psi$ components of circulation average zero in time; thus, these components may be neglected. The vertical induced velocities over the remainder of the disk are antisymmetric about the longitudinal axis. Thus, the average contribution over the entire rotor is zero.

Circumferential Vorticity

Equation (4) of reference 7 gives (noting that in the present case $d\Gamma/dL$ may be a function of ψ)

$$w_c = \frac{R}{4\pi} \int_0^{2\pi} \left(\frac{d\Gamma}{dL}\right) \frac{\left[(x \cos \psi + y \sin \psi - R) - \sin \chi \cos \psi \sqrt{R^2 + x^2 + y^2 + z^2 - 2R(x \cos \psi + y \sin \psi)}\right] d\psi}{\left[\sqrt{R^2 + x^2 + y^2 + z^2 - 2R(x \cos \psi + y \sin \psi)} + z \cos \chi - x \sin \chi + R \sin \chi \cos \psi\right] \sqrt{R^2 + x^2 + y^2 + z^2 - 2R(x \cos \psi + y \sin \psi)}} \tag{20}$$

For the center of the rotor, $x = y = z = 0$, so that equation (20) reduces to

$$w_c = -\frac{1}{4\pi} \int_0^{2\pi} \left(\frac{d\Gamma_0}{dL} + \frac{d\Gamma_1}{dL} \sin \psi\right) d\psi \tag{21}$$

from which

$$w_c = -\frac{1}{2} \frac{d\Gamma_0}{dL} \tag{22}$$

Equation (22) shows that the $\sin \psi$ component of the circumferential vorticity has no effect at the rotor center. The method of the next section can be used to show further that the effect of the $\sin \psi$ component is antisymmetric about the longitudinal axis so that it has no effect on the average value of induced velocity for the entire disk.

The symmetry theorems of reference 5 can be applied to show that equation (21) also gives the average induced velocity over the disk for a uniformly loaded rotor. Notice that the sum of the induced velocities of points located symmetrically about the lateral axis is constant and equal to twice the induced velocity at the lateral axis. Thus, the average velocity along any line in the disk, parallel to the longitudinal axis (that is, in the direction of flight), is equal to the induced velocity at the intercept of this line on the lateral axis. However, the induced velocity on the lateral axis is uniform and equal to that at the center of the rotor. Thus, the value of induced velocity (eq. (22)) at the center is identically equal to the average over the entire rotor.

Radial Vorticity

Choose a point P in the X-Z plane (fig. 7) about which the radial vorticity, being proportional to $\cos\psi$, is symmetrical. Now consider the vorticity in any plane through the wake and parallel to the tip path plane. Observe that for each radial element of vorticity in this plane, say 1, there is a corresponding element, 2, which exactly cancels the velocity induced by 1 in the X-Z plane. Thus, the velocity induced in the longitudinal plane is zero. Notice too, that the flow will be antisymmetric about the longitudinal axis so that the net contribution to the average induced velocity is also zero.

Axial Vorticity

The induced velocity contribution of the axial vorticity may be found by using the Biot-Savart law and integrating over the entire wake; thus,

$$d\bar{q}_a = \frac{\Gamma}{4\pi}\frac{d\bar{s}\times\bar{a}}{|\bar{a}|^3} \tag{23}$$

where (see fig. 8)

$$\bar{s} = \bar{i}(R\cos\psi + L) + \bar{j}(R\sin\psi) + \bar{k}(0) \tag{24a}$$

$$d\bar{s} = \left[\bar{i}(1) + \bar{j}(0) + \bar{k}(0)\right]dL \tag{24b}$$

$$\bar{a} = \bar{i}(R\cos\psi + L - x) + \bar{j}(R\sin\psi - y) + \bar{k}(-z) \tag{24c}$$

Substitution of equations (24b) and (24c) into equation (23) yields (for the center of the rotor)

$$d\bar{q}_a = \frac{-\dfrac{d\Gamma}{d(R\psi)}\begin{vmatrix} \bar{i} & \bar{j} & \bar{k} \\ 1 & 0 & 0 \\ (R\cos\psi + L) & R\sin\psi & 0 \end{vmatrix} dL\, d(R\psi)}{4\pi\left[(R\cos\psi + L)^2 + R^2\sin^2\psi\right]^{3/2}} \tag{25}$$

L
7
5
8

Note that $\dfrac{d\Gamma}{d(R\psi)} = \mu\left(\dfrac{d\Gamma_0}{dL} + \dfrac{d\Gamma_1}{dL}\sin\psi\right)$ (eq. (18)). Therefore, the vertical (or $\bar{k}$) component of induced velocity is

$$w_a = \frac{-\mu R}{4\pi}\int_0^{2\pi}\int_0^{\infty}\left(\frac{d\Gamma_0}{dL} + \frac{d\Gamma_1}{dL}\sin\psi\right)\frac{R\sin\psi\, dL\, d\psi}{\left(R^2 + 2RL\cos\psi + L^2\right)^{3/2}} \tag{26}$$

Equation (26) may be integrated with respect to L by means of item 162 of reference 8. Thus, after inserting the limits of integration

$$w_a = \frac{-\mu}{4\pi}\int_0^{2\pi}\left(\frac{d\Gamma_0}{dL} + \frac{d\Gamma_1}{dL}\sin\psi\right)\frac{1 + \cos\psi}{\sin\psi}\, d\psi \tag{27}$$

which may be rewritten as

$$w_a = \frac{-\mu}{4\pi}\frac{d\Gamma_0}{dL}\int_0^{2\pi}\frac{\sin\psi}{1 - \cos\psi}\, d\psi - \frac{\mu}{4\pi}\frac{d\Gamma_1}{dL}\int_0^{2\pi}(1 + \cos\psi)d\psi \tag{28}$$

Notice that $\dfrac{\sin\psi}{1 - \cos\psi}$ is discontinuous at $\psi = 0$ and 2π. Therefore, rewrite equation (28) as

$$w_a = \frac{-\mu}{4\pi}\frac{d\Gamma_0}{dL}\left(\lim_{\epsilon\to 0}\int_{\epsilon}^{2\pi-\epsilon}\frac{\sin\psi}{1 - \cos\psi}\, d\psi\right) - \frac{\mu}{4\pi}\frac{d\Gamma_1}{dL}\int_0^{2\pi}(1 + \cos\psi)d\psi \tag{29}$$

The integration with respect to ψ is carried out with the aid of item 303 of reference 8 to yield

$$w_a = \frac{-\mu}{4\pi}\frac{d\Gamma_0}{dL}\left(\lim_{\epsilon\to 0}\left\{\log\left[\frac{1 - \cos(2\pi - \epsilon)}{1 - \cos\epsilon}\right]\right\}\right) - \frac{\mu}{2}\frac{d\Gamma_1}{dL} \tag{30}$$

which becomes, after the limiting process

$$w_a = -\frac{\mu}{2}\frac{d\Gamma_1}{dL} \tag{31}$$

The induced velocity due to axial vorticity will be symmetrical about the longitudinal axis of the rotor and its mean value is therefore not zero. Instead, a mean upwash is imposed upon the rotor. That part of the far wake caused by the axial vorticity is identical to the wake of an elliptically loaded (uniform downwash) wing. Thus, the induced velocity given by equation (31) will be the average induced velocity as well as the induced velocity at the center of the rotor.

TOTAL INDUCED VELOCITY AT CENTER OF ROTOR

Uniform Loading

For the case of uniform loading, where $\Gamma_1 = 0$, it may be seen that the only portion of the wake which contributes an induced velocity at the center of the rotor is the circumferential vorticity. This induced velocity is given by equation (22) as

$$w = w_c = -\frac{1}{2}\frac{d\Gamma_0}{dL}$$

or substituting for $d\Gamma_0/dL$ from equation (17),

$$w = \frac{-\frac{1}{2}C_T\Omega R}{\sqrt{\mu^2 + \lambda^2}} \tag{32}$$

With Sin ψ Loading

In the case of $\sin\psi$ loading there will be an additional term, given by equation (31), in the induced velocity at the center of the rotor. Thus,

$$w = w_c + w_a \tag{33}$$

and from equations (22) and (31)

$$w = -\frac{1}{2}\frac{d\Gamma_0}{dL} - \frac{\mu}{2}\frac{d\Gamma_1}{dL} \tag{34}$$

In equation (34), substitute the values of $d\Gamma_0/dL$ and $d\Gamma_1/dL$ from equations (15) and (16) to obtain

$$w = \frac{-\frac{1}{2}C_T\Omega R}{\left(1 - \frac{3}{2}\mu^2\right)\sqrt{\mu^2 + \lambda^2}} + \frac{\frac{3}{4}\mu^2 C_T\Omega R}{\left(1 - \frac{3}{2}\mu^2\right)\sqrt{\mu^2 + \lambda^2}} \tag{35}$$

or

$$w = \frac{-\frac{1}{2}C_T\Omega R}{\sqrt{\mu^2 + \lambda^2}} \tag{36}$$

which, because of the symmetries previously discussed, will be the average or mean induced velocity, for the rotor as well as the induced velocity at the center of the rotor.

Notice that reference 4, which assumes a $\sin\psi$ circulation but which ignores axial vorticity, obtains only the first term of equation (35), or

$$w = \frac{-\frac{1}{2}C_T\Omega R}{\left(1 - \frac{3}{2}\mu^2\right)\sqrt{\mu^2 + \lambda^2}} \tag{37}$$

DISCUSSION

CORRESPONDENCE OF THEORIES

Comparison of equations (2), (32), and (36) indicates that, regardless of whether or not the blade circulation is allowed to vary as $\sin \psi$, vortex theory yields precisely the same induced velocity as momentum theory. The term $\frac{1}{1 - \frac{3}{2}\mu^2}$, obtained in reference 4, is not as it has often been described, a correction to account for lateral dissymmetry. Instead it is simply introduced by neglect of the axial vorticity.

It will be noted that equation (9) indicates that inclusion of the lateral dissymmetry ($\sin \psi$ term) has reduced the thrust for a given value of the constant circulation Γ_0. This effect, however, is exactly counterbalanced by the reduction of downwash resulting from the axial vorticity.

CONSISTENT SETS OF ASSUMPTIONS

It would appear from the analysis that there is a considerable difference in the manner in which certain assumptions in the development have been described. In particular, the assumption that the vortex filaments are very closely spaced on the wake cylinder has been in the past interchangeably described as equivalent to an infinite tip speed or to an infinite number of blades. With infinite tip speed, the forward and induced velocities are both negligible in comparison with the rotational speed. Thus, the vortex filaments will lie essentially as rings on the cylinder (as in fig. 3(b)); Γ_1 will approach zero; and the axial component will, indeed, be negligible. On the other hand, with an infinite number of blades, the forward and induced velocities are not negligible. Thus, Γ_1 does not approach zero, and the vortex filaments lie on the wake cylinder as spirals so that the axial component of vorticity must be considered. The failure to use a consistent set of these assumptions can yield an incorrect result, as shown by equation (37).

LATERAL VARIATION OF INDUCED VELOCITY

It will be noted that the present paper, under the simplifications possible when considering only the center of the rotor, treats certain parts of the wake by different techniques than those used in reference 4. For example, reference 4 assumes that the combined effect of the radial vorticity may be found by superposing two smaller cylinders originating from a blade circulation of $\Gamma_1 = \pm \frac{3}{2} \mu\Gamma_0$ within the main wake (fig. 9). It will be observed that the effect of these two inner cylinders cancel exactly at the center of the rotor, just as the effect of this part of the wake does in the present analysis. Reference 4 progresses further, however, to obtain an approximation to the lateral distribution of induced velocity by numerically computing the induced velocities at $r/R = \pm 0.75$. These numerical values were then used to determine a "slope" of induced velocity along the lateral axis. It has since become evident, however, from the theorems of reference 5, that if the external field of each of the smaller cylinders is neglected, then the induced velocity across the lateral axis of either small cylinder must be uniform. Thus, under the assumptions of reference 4, the variation of induced velocity on the lateral axis of the rotor should not have been linear, but rather, almost uniform on either side of the center. It will be noted, however, that components of the wake other than those considered in this section also have an effect on the lateral variation of induced velocity. A complete analysis is considered beyond the scope of the present paper.

CONCLUSIONS

This study of the induced velocity of a helicopter rotor has shown that:

1. Momentum theory and vortex theory yield precisely the same value whether or not the blade circulation is allowed to vary as the sine of the azimuth angle.

2. It is necessary to use a consistent set of assumptions in dealing with the induced velocity by means of vortex theory, in particular, if the lateral dissymmetry of the rotor is represented by blade circulation which varies as the sine of the azimuth angle, it is necessary to include the axial component of vorticity in the calculations.

Langley Research Center,
National Aeronautics and Space Administration,
Langley Field, Va., December 15, 1959.

REFERENCES

1. Glauert, H.: A General Theory of the Autogyro. R. & M. No. 1111, British A.R.C., 1926.

2. Glauert, H.: Airplane Propellers. Helicopter Airscrews. Vol. IV of Aerodynamic Theory, div. L, ch. X, sec. 5, W. F. Durand, ed., Julius Springer (Berlin), 1935, p. 319.

3. Coleman, Robert P., Feingold, Arnold M., and Stempin, Carl W.: Evaluation of the Induced-Velocity Field of an Idealized Helicopter Rotor. NACA WR L-126, 1945. (Formerly NACA ARR L5E10.)

4. Drees, J. Meijer: A Theory of Airflow Through Rotors and Its Application to Some Helicopter Problems. Jour. Helicopter Assoc. of Great Britain, vol. 3, no. 2, July-Aug.-Sept. 1949, pp. 79-104.

5. Heyson, Harry H., and Katzoff, S.: Induced Velocities Near a Lifting Rotor With Nonuniform Disk Loading. NACA Rep. 1319, 1957. (Supersedes NACA TN 3690 by Heyson and Katzoff and TN 3691 by Heyson.)

6. Gessow, Alfred, and Myers, Garry C., Jr.: Aerodynamics of the Helicopter. The Macmillan Co., c.1952, p. 193.

7. Heyson, Harry H.: Jet-Boundary Corrections for Lifting Rotors Centered in Rectangular Wind Tunnels. NASA TR R-71, 1960.

8. Peirce, B. O.: A Short Table of Integrals. Third rev. ed., Ginn and Co., 1929, pp. 24-42.

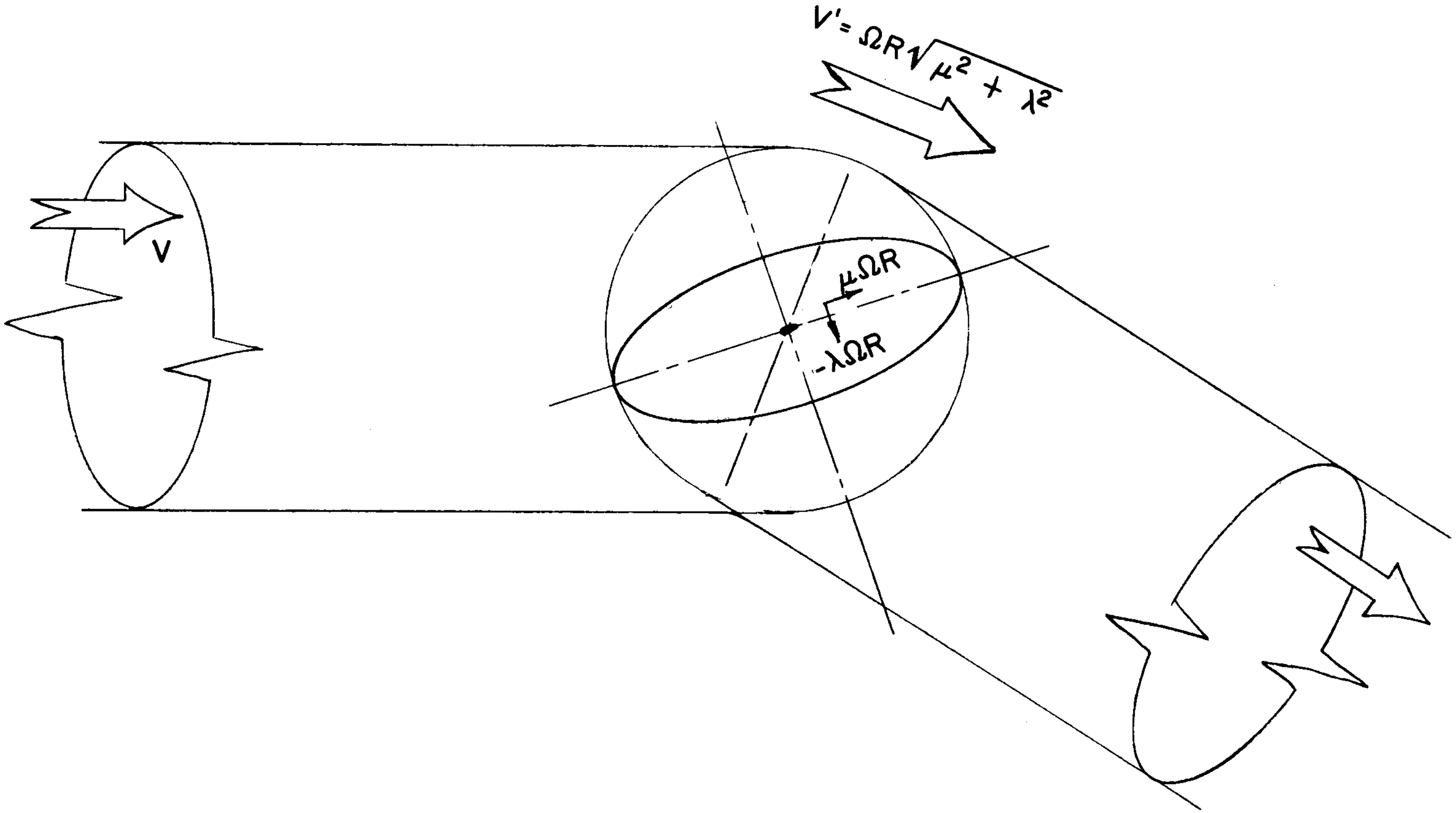

Figure 1.- Sketch for determining induced velocity by means of momentum theory.

L-758

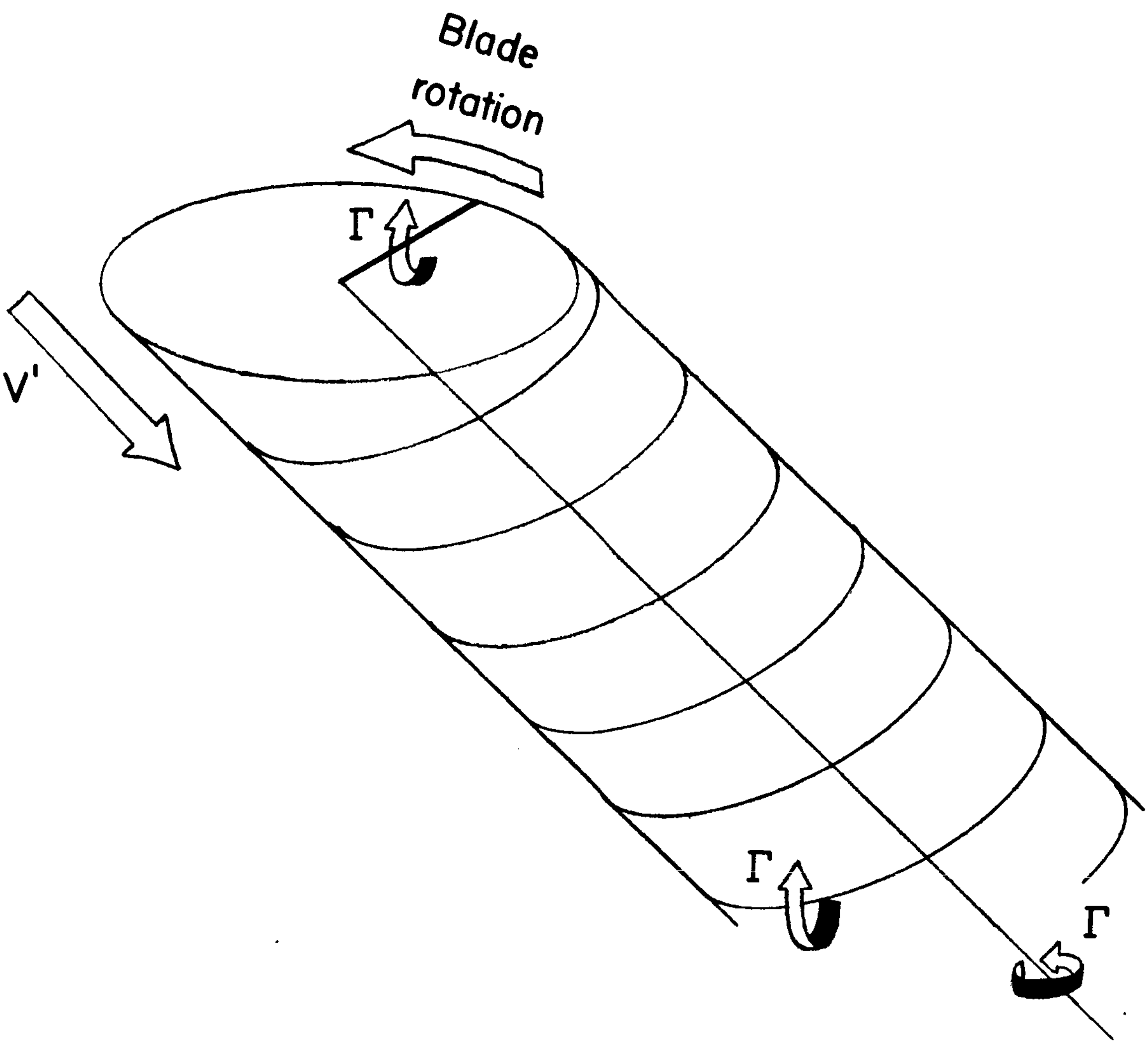

Figure 2.- Schematic view of vortices in rotor wake.

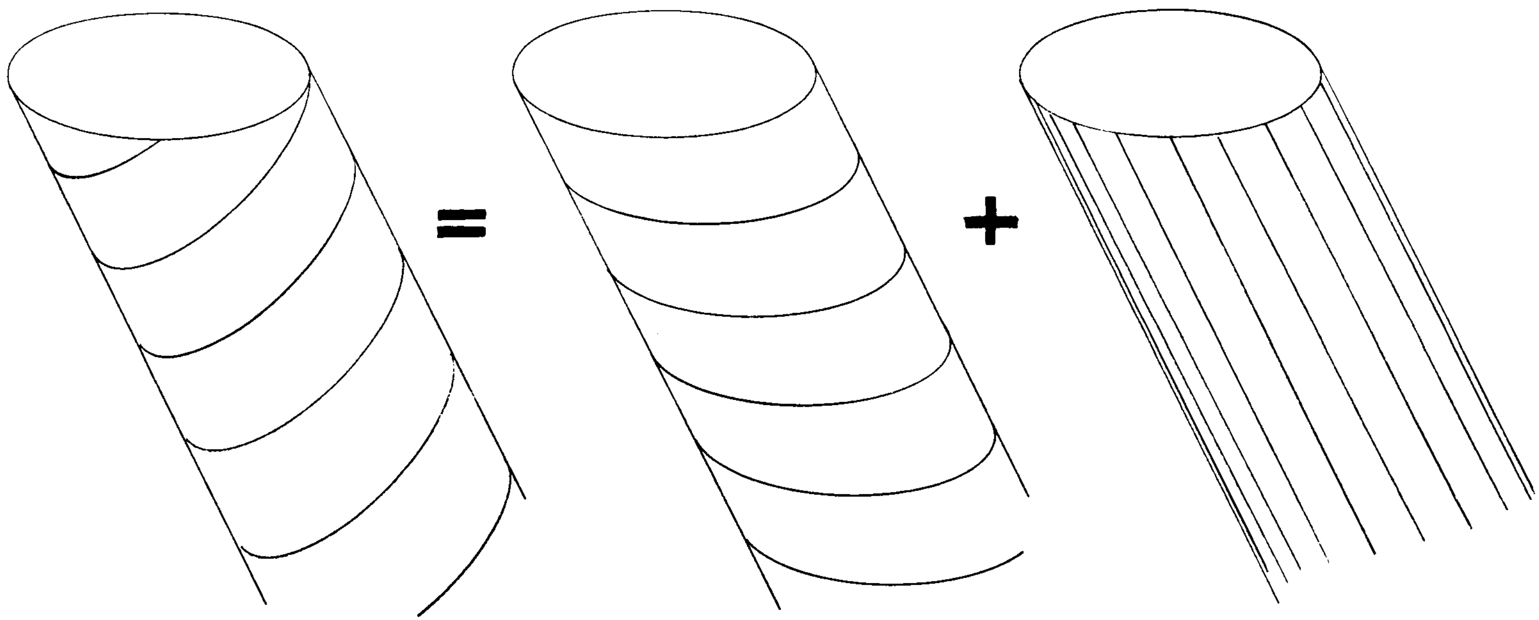

(a) Outer vortex wake.

(b) Circumferential component.

(c) Axial component.

Figure 3.- Decomposition of cylindrical wake into circumferential (vortex ring) and axial components.

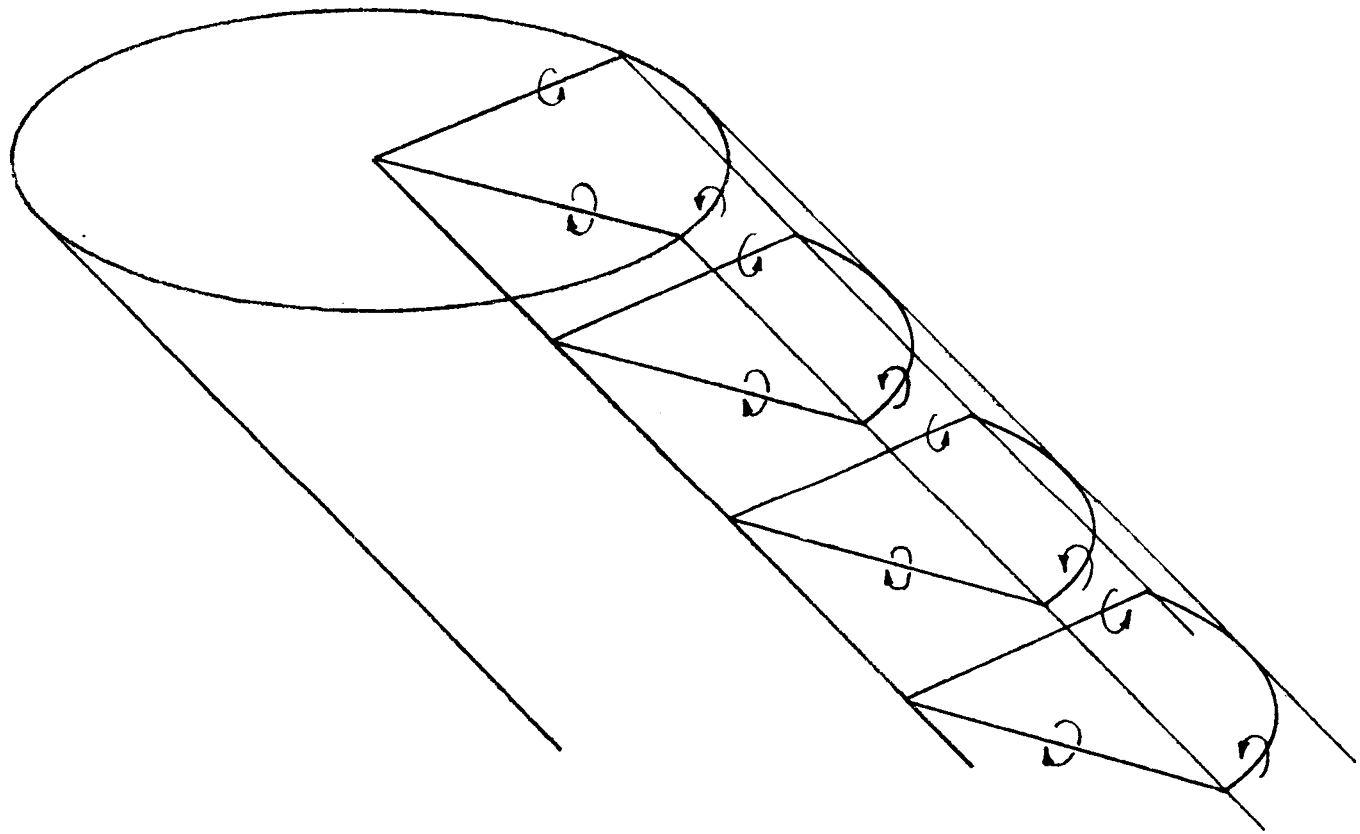

Figure 4.- Radial vorticity left as a result of a step change in lift over a sector of the rotor disk.

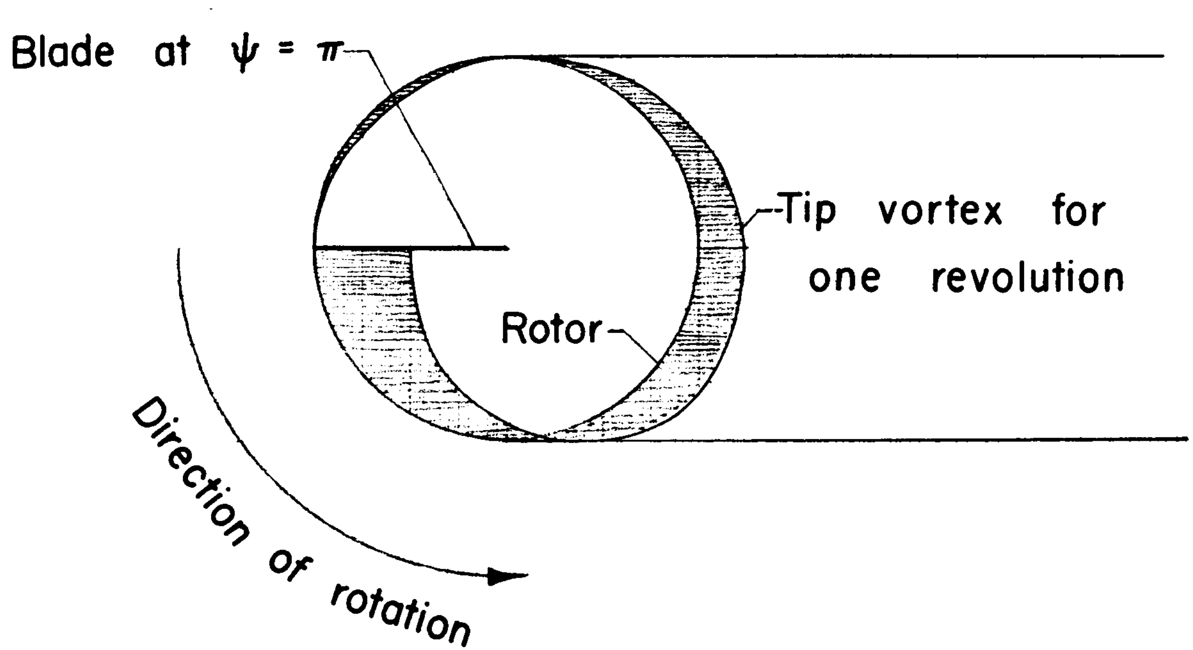

(a) Rotor wake at $\chi = 90^{\circ}$.

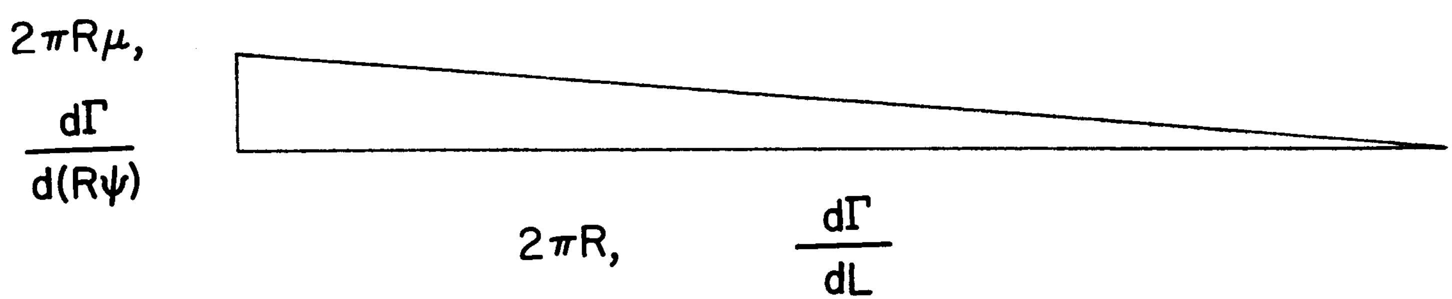

(b) Developed triangle.

Figure 5.- Sketches for determining strength of axial vorticity.

L-758

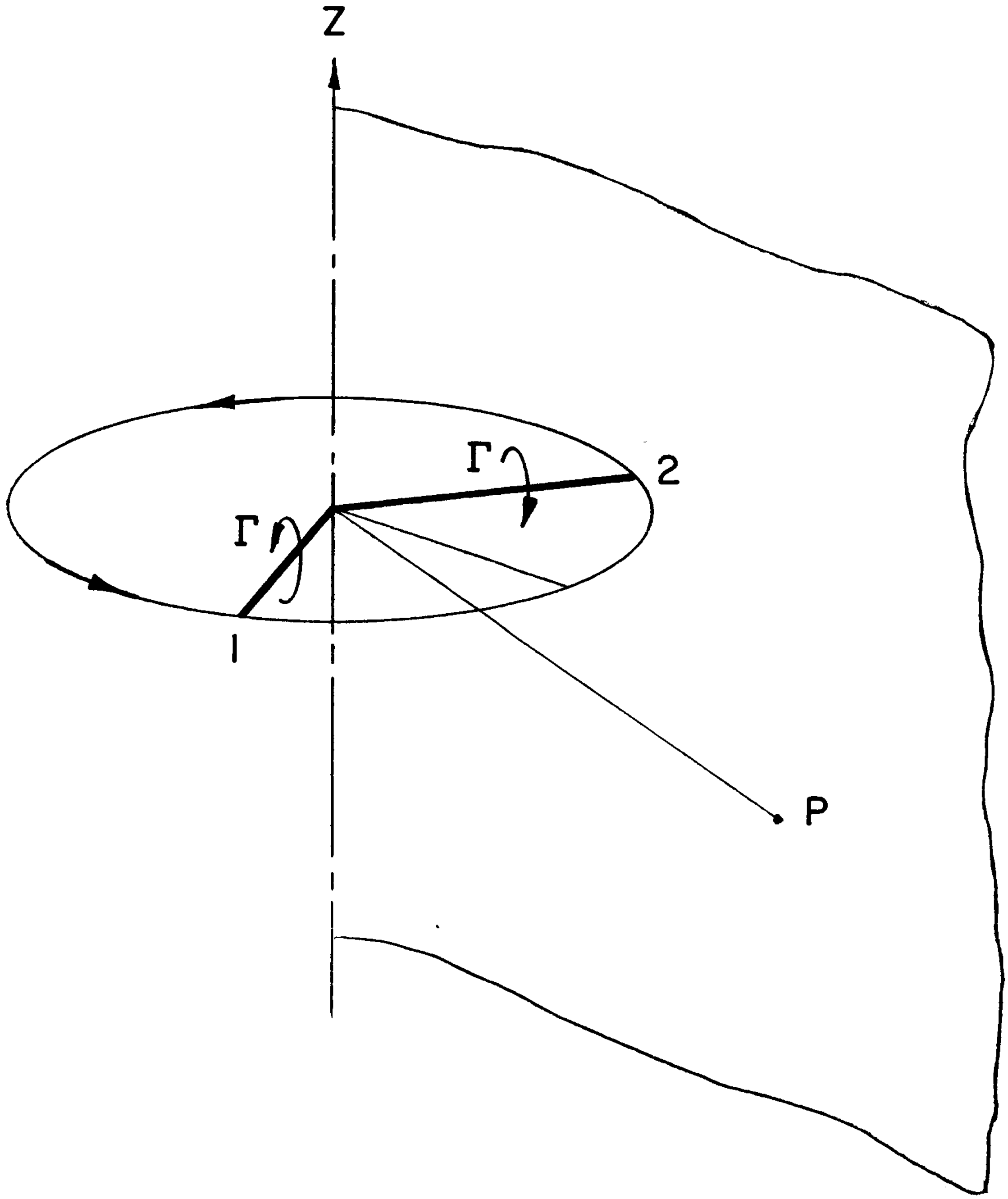

Figure 6.- Sketch for determining effect of blade circulation on induced velocities.

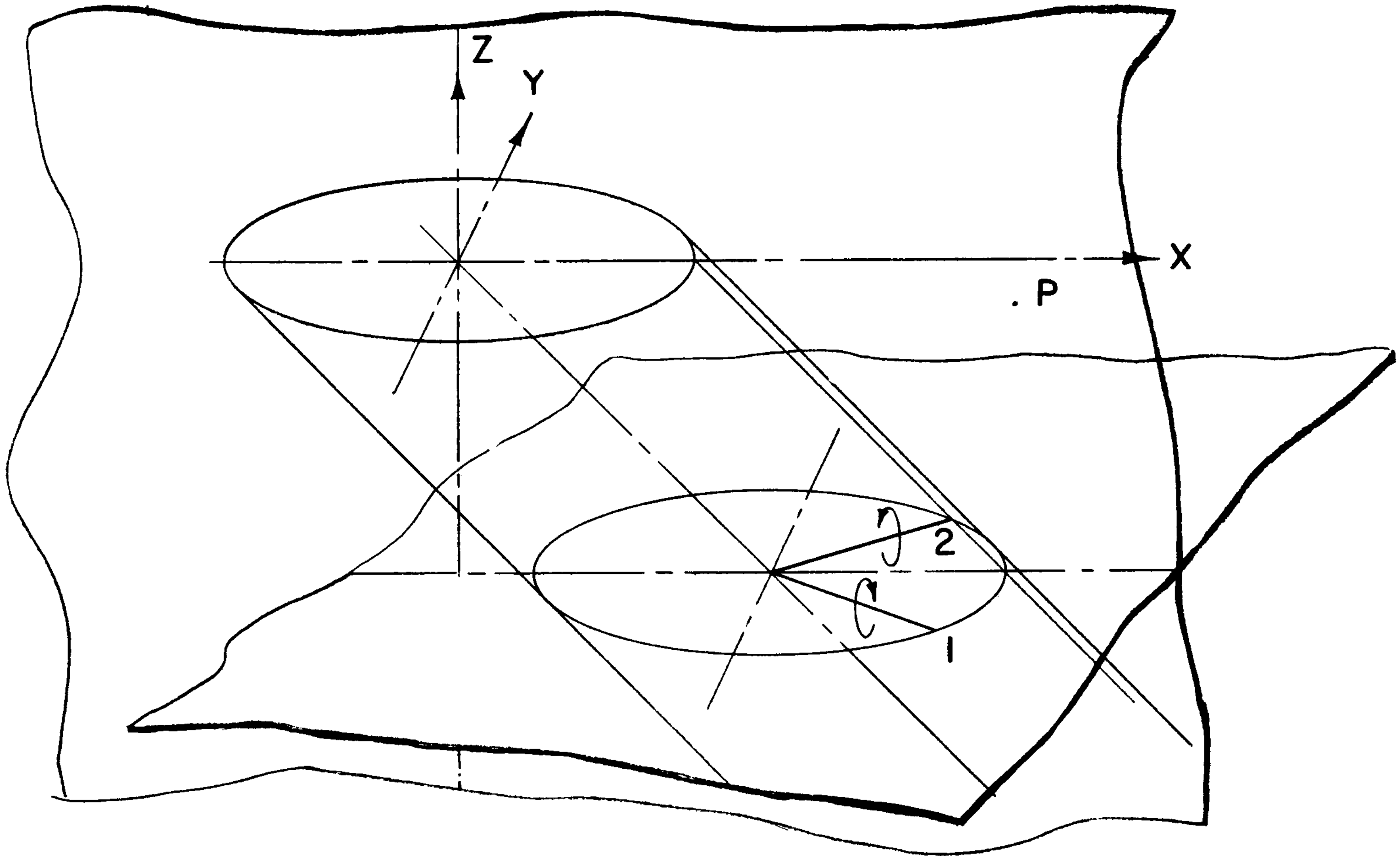

Figure 7.- Sketch for determining effect of radial vorticity on induced velocities.

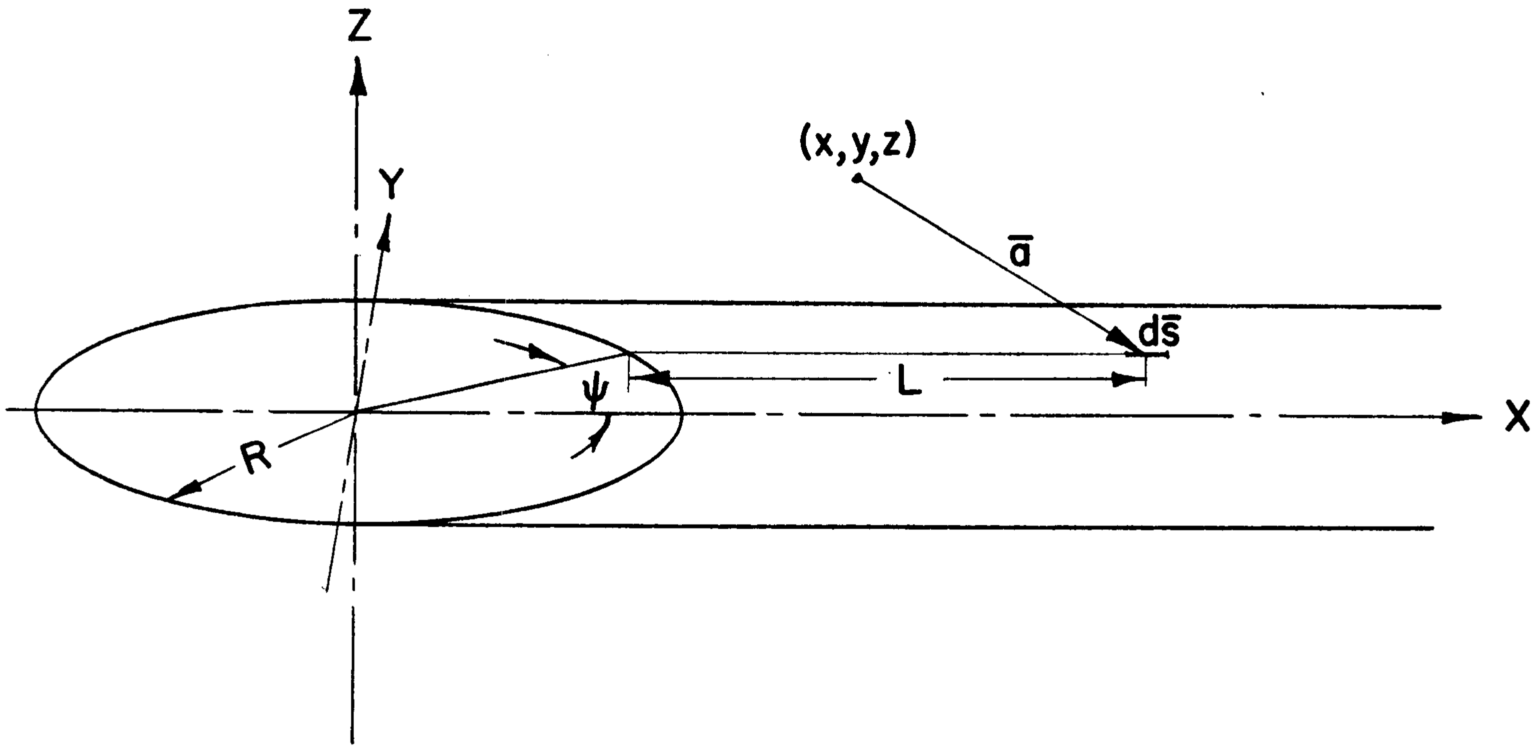

Figure 8.- Geometric arrangement of axial vorticity in wake.

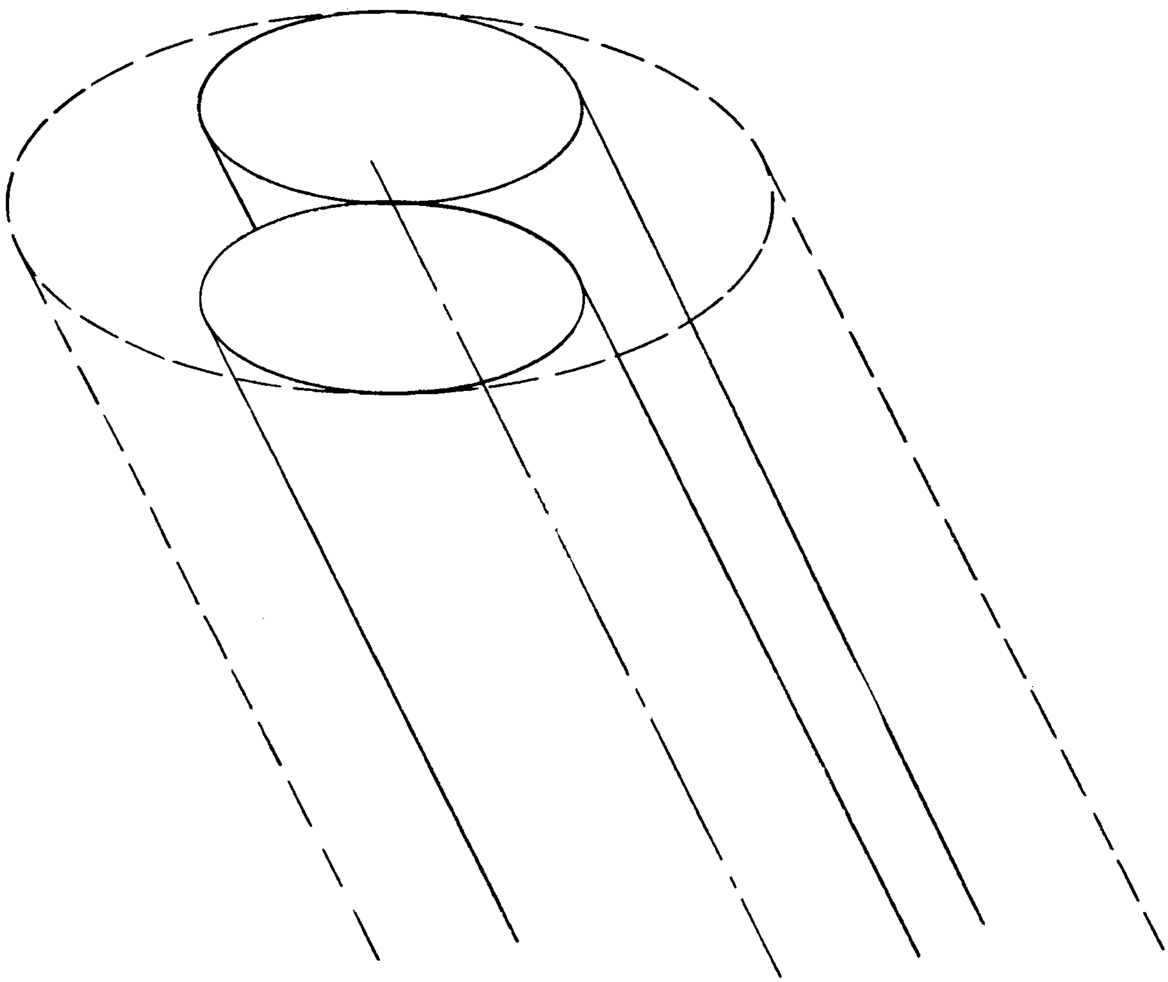

Figure 9.- Vortex configuration used in reference 4 to represent the combined effect of radial and sin ψ circumferential vorticity.